Effect of interpolation kernels and grid refinement on two way–coupled point-particle simulations

By S. V. Apte†, N. Keane‡, S. S. Jain AND M. A. Khanwale

In this study, a two way–coupled point-particle Euler-Lagrange model is used to evaluate particle-turbulence interactions at low-volume loadings in decaying isotropic turbulence laden with Kolmogorov-scale particles. Particle-fluid interactions are modeled using standard drag law for this large density-ratio system. The decay rates in kinetic energy and dissipation are evaluated with and without considering the self-disturbance effect created by the particles to obtain the undisturbed fluid velocity needed in the drag closure. Different interpolation kernels that vary based on local grid resolution and particle size are evaluated through a systematic grid-refinement study. We find that the interpolation kernel widths that scale based on the particle size perform significantly better under grid refinement than kernels based on the grid resolution.

1. Introduction

In two way–coupled point-particle (PP) models used for particle-laden flows, the particles are typically assumed to be spherical, subgrid (much smaller than the smallest resolved scales of fluid motion), with low volume loading, and modeled as point sources. The dynamics of the particles are captured by solving the Maxey-Riley equation with closure models for drag, lift, added mass, pressure, and history forces, among others (Maxey 1987). The reaction force from the particles is added to the fluid momentum equations. In low-volume loadings, the particle force closures are based on the relative slip velocity at the particle location, which involves the difference between the undisturbed fluid velocity and the particle velocity. The undisturbed fluid velocity seen by the particle is defined as the fluid velocity seen by the particle in the absence of the self-disturbance field created by the particle. However, in a two way–coupled point-particle model, the particle affects the fluid flow in its neighborhood, and thus the undisturbed fluid velocity is not readily available. It is standard practice to simply use the two way–coupled fluid velocity to compute the closure forces (Apte *et al.* 2003).

When the particle size is very small compared to the grid resolution ($D_p \ll \Delta$), where D_p is the particle diameter and Δ is the grid size, the above approximation does not result in any significant error. However, when the particle size is comparable to the grid size ($D_p \sim \Delta$), because of such an approximation, significant errors in particle and fluid statistics are reported, especially at low particle Reynolds numbers (Gualtieri *et al.* 2015; Horwitz & Mani 2016, 2018; Esmaily & Horwitz 2018; Fukada *et al.* 2018). Recent work initiated by Horwitz & Mani (2016) and Esmaily & Horwitz (2018) followed by several other researchers (Liu *et al.* 2019; Pakseresht *et al.* 2020; Pakseresht & Apte 2021; Apte 2022) has led to the development of new schemes and models to recover the undisturbed fluid velocity with improved predictions in capturing the particle-turbulence interactions

† School of Mechanical, Industrial, and Manufacturing Engineering, Oregon State University
‡ College of Earth, Ocean, and Atmospheric Sciences, Oregon State University

in homogeneous, isotropic turbulence (Mehrabadi *et al.* 2018) and wall-bounded channel flows (Horwitz *et al.* 2022).

Recently, Horwitz & Mani (2020) conducted a detailed evaluation of numerics and grid resolution on fluid-particle interactions predicted by point-particle models, with and without correcting for the particle self-disturbance field, in homogeneous isotropic turbulence. For a particle size to a Kolmogorov-scale ratio (D_p/η) of 0.25, the grid resolution (D_p/Δ) was refined over the range of 0.25–1 and statistics of fluid kinetic energy, dissipation rate, particle kinetic energy, and particle acceleration were evaluated in detail. Different interpolation kernels, e.g., trilinear, fourth-order Lagrange, and cubic splines, for Euler-to-Lagrange (E2L) and Lagrange-to-Euler (L2E) interpolation were used. All the interpolation kernels have grid-based interpolation stencils. As the grid is refined, the interpolation stencil becomes narrower, localizing the effect of the particle on the fluid and vice versa. It was found that, in the absence of any correction model for self-disturbance, the fluid and particle statistics do not result in grid-converged solutions. The fluid-particle interactions were better predicted when the grid is coarser, and hence neglecting the self-disturbance effect resulted in a smaller error on coarser grids. With grid refinement, the self-disturbance field is stronger, as the particle reaction force is distributed over a smaller region due to localized interpolation kernels, resulting in a larger error. In contrast, when a correction model was used to obtain the undisturbed fluid velocity, consistent results were obtained for all kernels as the grid was refined, emphasizing the importance of self-disturbance correction, especially when the particle size is comparable to the grid resolution and grid-based interpolation kernels are used.

The grid-based interpolation kernels discussed above are commonly used because they provide compact support for the E2L and L2E interpolations. For example, in trilinear interpolation, only the nearest neighbors of a grid cell are necessary for the interpolation, making them straightforward to implement for complex, arbitrary-shaped grids. In addition, the E2L and L2E interpolation functions are typically identical, following the kinetic energy conservation principles identified by Sundaram & Collins (1996), to ensure correct behavior of the overall energy balance in the limit of $D_p \ll \Delta$.

The present work focuses on two main hypotheses when particle sizes are comparable to the grid resolution ($D_p \sim \Delta$). First, the kernel width used in E2L and L2E interpolations should scale with the particle size and should be independent of the grid resolution. This keeps the region of influence of the particle the same, irrespective of the grid resolution. Second, using a larger kernel width for E2L interpolation with a wider stencil will sample the fluid velocity from a region with reduced influence from the self-disturbance field, thus improving the estimate of the fluid velocity at the particle location even without any correction model. However, a localized kernel for L2E with narrow width may be able to capture the reaction of the particle on the fluid more accurately. This suggests the use of nonsymmetric interpolation kernels for E2L and L2E interpolations, especially in the absence of any correction for the self-disturbance.

To test these hypotheses, a detailed study of particle-turbulence interactions is conducted using three different interpolation kernels and four grid resolutions while keeping all other fluid and particle parameters the same. Three interpolation functions include a grid-based Roma-delta. function independent of the particle size and Gaussian kernels with two different kernel widths that scale with the particle size. The Roma-delta function is a compact, grid-based, second-order interpolation commonly employed in direct forcing–based immersed-boundary methods, whereas Gauss1 ($\sigma = D_p\sqrt{2/\pi}$) and Gauss2 ($\sigma = 1.5D_p$) are Gaussian kernel functions with kernel width σ that scales with

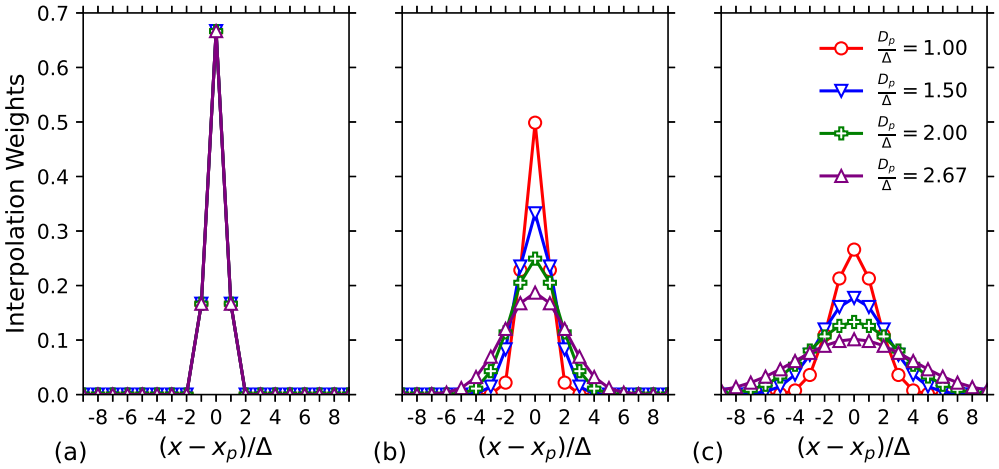

FIGURE 1. Interpolation weight distribution with grid refinement keeping the particle size unchanged: (a) Roma, (b) Gauss1, and (c) Gauss2.

the particle diameter D_p. The Gauss1 kernel is commonly used in force-coupling methods (Lomholt *et al.* 2002), wherein σ is chosen such that the fluid velocity at the particle location matches the rigid-body motion of the particle, approximately enforcing a boundary condition at the particle location (Gualtieri *et al.* 2015). The Gauss2 kernel width is similar to the polynomial function used by Deen *et al.* (2009).

Figure 1 shows the comparison of weights under grid refinement for these three interpolation kernels. The Roma-delta function results in the same weights for neighboring grid points with grid refinement and is independent of the particle size. This makes the two-way coupling force distribution (L2E) and interpolation of the fluid velocity at particle location (E2L) highly localized as the grid is refined. Such a kernel is sufficient when the particle is much smaller than the grid resolution; however, it can give rise to a large disturbance field for $D_p \sim \Delta$, as the reaction force from the particle is distributed in a very narrow region. The Gauss1 and Gauss2 kernels show weight distributions over a region of interest surrounding the particle that scales with the particle size. As the grid resolution becomes finer than the particle size, the interpolation weights are spread over more neighboring control volumes spanning over a σ proportional to the D_p. However, when the particle becomes much smaller than the grid resolution (not shown), this kernel will produce a sharp delta function at the particle location, resulting in zero or very small weights at the grid point. Under such circumstances, a grid-based Roma interpolation kernel may be more suitable for obtaining a smoother transition with particle motion.

In this work, starting with particle size on the order of the grid resolution, evaluation of point-particle models with and without self-disturbance correction is conducted under grid refinement, wherein the particle size becomes larger than the grid resolution. Results obtained from the grid-based Roma interpolation kernel are compared with those obtained from Gauss1 and Gauss2. For these cases, the E2L and L2E interpolation functions are identical. To test the second hypothesis, different interpolation kernels with a narrower kernel of Roma-delta function for L2E and a wider kernel of Gauss2 for E2L are used (denoted as Roma-Gauss2).

In Section 2, a brief description of the zonal advection-diffusion-reaction (Zonal-ADR) model for self-disturbance correction is provided. Results for flow over a stationary par-

ticle and then particle-laden decaying isotropic turbulence corresponding to the particle-resolved direct numerical simulation (PR-DNS) study of Mehrabadi *et al.* (2018) are summarized in Section 3, followed by conclusions in Section 4.

2. Mathematical formulation

The core idea behind the Zonal-ADR model for obtaining the undisturbed fluid velocity in point-particle simulations is summarized here [see Apte (2022) for details]. The self-disturbance created by a particle is approximated by the following differential equation

$$\rho_g \frac{\partial u_i^d}{\partial t} + \rho_g \frac{\partial \left(u_j u_i^d\right)}{\partial x_j} = \left(K_\mu \mu\right) \frac{\partial^2 u_i^d}{\partial x_j^2} - \dot{S}_i, \tag{2.1}$$

where ρ_g is the fluid density, and $K_\mu \mu = 1.5\mu$ is the effective viscosity designed to match the disturbance field in the Stokes limit. The same value of K_μ is found to give good results even for higher-particle Reynolds numbers (up to 100). The superscript $(\cdot)^d$ corresponds to the disturbance field, $+(\dot{S}_i)$ is the particle reaction force on the fluid, and u_j without any superscript is the two way–coupled velocity field that is affected by the self-disturbances of all particles. Knowing u_j, the disturbance field is solved for each particle in a small region of interest surrounding the particle, using an overset-mesh-like formulation. The undisturbed fluid velocity is then obtained as $u_i^{un} = u_i + u_i^d$. The implementation of this zonal approach in a collocated, second-order, fractional time-stepping solver is described in Apte (2022) with detailed verification studies.

3. Results

The Zonal-ADR correction method is used to investigate the particle-turbulence interactions in decaying isotopic turbulence corresponding to the PR-DNS study of Mehrabadi *et al.* (2018), which involves Kolmogorov-scale particles. To understand the effect of different kernels and kernel widths for E2L and L2E interpolations, a simple test case of a stationary particle in a uniform flow is investigated at parameters (Reynolds number, ratio of D_p to Δ) representative of those in the isotropic turbulence case.

3.1. *Flow over a stationary sphere*

In this section, flow over a stationary particle is investigated at a particle Reynolds number (Re_p) of 1, which is representative of the Reynolds numbers obtained in the isotropic turbulence case discussed later in Section 3.2. A particle of size $D_p = 2\pi/96$ is placed at the center of a cubic domain of length 2π. A grid resolution of $\Delta = D_p = 2\pi/96$ is used for baseline computations. A systematic grid refinement study, keeping the particle parameters the same, is carried out with grid sizes of $2\pi/48$, $2\pi/96$, $2\pi/192$, and $2\pi/256$. The main goal of this study is to quantify the effect of grid refinement on predicting the drag force on the particle using different interpolation kernels, namely, (i) Roma, (ii) Gauss1, (iii) Gauss2, and (iv) Roma-Gauss2. The E2L and L2E interpolation functions are the same for the first three cases, whereas the Roma-Gauss2 uses the Roma function for L2E and Gauss2 for E2L interpolations.

Table 1 shows the relative error in computing the undisturbed fluid velocity at the particle location ($u_{@p}^{un}$) with and without the Zonal-ADR correction, compared to the true value [corresponding to the inlet velocity (u_{in}) of 1], the relative error in the particle drag force F_p, and the actual disturbed two way–coupled velocity at the particle

D_p/Δ	Interpolation	No Correction			Zonal-ADR		
		% Relative Error		$u^{2w}_{@p}/u_{in}$	% Relative Error		$u^{2w}_{@p}/u_{in}$
		$u^{un}_{@p}$	F_p		$u^{un}_{@p}$	F_p	
0.5	Roma	16.3	17.56	0.84	1.24	1.36	0.798
0.5	Gauss1	16.3	17.5	0.837	0.83	1.35	0.882
0.5	Gauss2	10.4	11.2	0.897	0.35	0.9	0.87
0.5	Roma-Gauss2	13.0	13.78	0.872	0.59	0.63	0.81
1	Roma	33.7	35.8	0.66	0.87	0.9	0.47
1	Gauss1	22.5	24.6	0.76	0.6	0.67	0.7
1	Gauss2	11.5	12.5	0.88	0.35	0.38	0.87
1	Roma-Gauss2	16.5	17.7	0.84	0.59	0.63	0.81
2	Roma	53.4	55.9	0.47	5.4	5.8	-0.16
2	Gauss1	23.1	24.6	0.77	0.1	0.1	0.3
2	Gauss2	13.8	14.9	0.86	0.9	0.98	0.83
2	Roma-Gauss2	19.6	21.3	0.8	0.13	0.16	0.25
2.66	Roma	60.9	63.32	0.39	7.1	7.6	-0.558
2.66	Gauss1	16.3	17.5	0.837	1.47	1.6	0.625
2.66	Gauss2	10.3	11.2	0.897	0.97	1.05	0.82
2.66	Roma-Gauss2	12.8	13.7	0.872	1.4	1.3	0.724

TABLE 1. Effect of grid refinement on undisturbed fluid velocity and particle drag force as well as the disturbed fluid velocity at the particle location for different interpolation kernels.

location normalized by the inlet velocity ($u^{2w}_{@p}/u_{\mathrm{in}}$). The errors in particle force and the undisturbed fluid velocity at the particle location are large (10–60%) and the errors get worse with grid refinement, especially when the grid-based Roma-delta function is used. This result is consistent with the main conclusions of Horwitz & Mani (2020), who used trilinear interpolation for particle-laden isotropic turbulence and observed that coarser meshes resulted in better predictions and the prediction errors became worse with grid refinement. As the grid is refined, the Roma kernel becomes narrower and distributes the particle reaction force to the nearest neighbors of the control volume containing the particle. This creates a strong disturbance field and, without any correction, results in a large error. With the Zonal-ADR correction, even for a grid-based Roma interpolation kernel, particle force and undisturbed fluid velocity errors are significantly smaller for all grid refinements. However, when the grid resolution is finer than the particle size, a negative two-way fluid velocity at the particle location is observed, which is unphysical based on flow around a particle obtained from particle-resolved simulations. This suggests that, with a very narrow interpolation kernel, a large particle reaction force creates an extremely strong disturbance resulting in negative fluid velocity at the particle location.

When the interpolation kernel width is based on the particle size (Gauss1 and Gauss2), the errors are reduced even when no correction is used and remain small under grid refinement. With the Zonal-ADR correction, the errors are significantly lower ($< 1.5\%$) compared to the Roma interpolation, and the two-way fluid velocity at the particle location does not become negative. Interestingly, even the Roma-Gauss2 (L2E-E2L) inter-

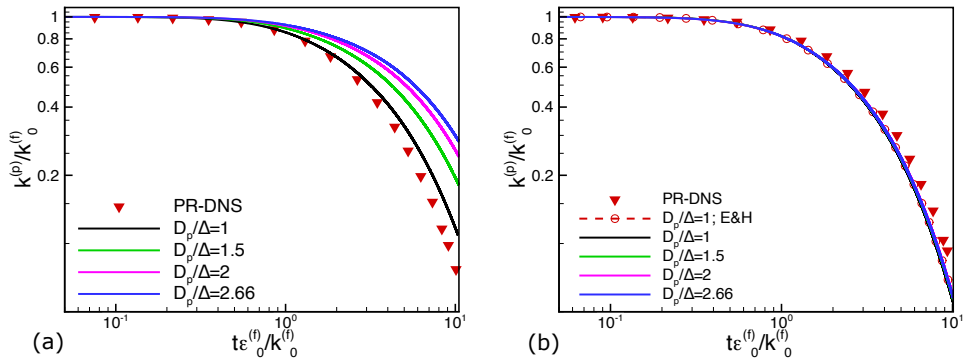

FIGURE 2. Temporal evolution of normalized particle kinetic energy under grid refinement with the grid-based Roma kernel for (a) no model, and (b) Zonal-ADR. E&H represents the result from Esmaily & Horwitz (2018) correction scheme implemented in the present collocated-grid solver. PR-DNS data is from Mehrabadi *et al.* (2018).

polation results in small errors compared to the Roma (L2E-E2L) kernel, even without the Zonal-ADR correction, although the errors are slightly larger than Gauss1 or Gauss2 kernels. This suggests that using a wider stencil, proportional to the particle size, to obtain the fluid velocity at the particle location samples the flow from a region less affected by the self-disturbance of the particle, resulting in better predictions. Numerical errors produced by not using the same interpolation stencils for L2E and E2L (Sundaram & Collins 1996) are compensated by better prediction of the undisturbed fluid velocity using particle-based kernels. However, symmetric (E2L-L2E) kernels, such as Gauss1 and Gauss2, generally give smaller errors.

3.2. *Decaying isotropic turbulence*

Particle-laden, decaying, isotropic turbulence corresponding to the particle-resolved data by Mehrabadi *et al.* (2018), at Taylor microscale Reynolds number of $Re_\lambda \approx 27$, is investigated. The computational domain is a triply periodic cubic box of side length 2π. The initial condition for each case is the divergence-free random field sampled from Pope's model energy spectrum (Pope 2000). The initial Kolmogorov length scale, η_0, is set to $2\pi/96$ and the energy spectrum parameters are based on Mehrabadi *et al.* (2018).

For the baseline case, the grid size (Δ) is selected to be the same as the initial Kolmogorov scale, which is equal to the particle size ($D_p = \eta_0$). The particle-to-fluid density ratio is $\rho_p/\rho_f = 1800$, and the volume and mass loading are $\phi = 0.001$ and $\phi_m = 1.8$, respectively, giving a total of $N_p = 1689$ particles in the domain. This results in a large particle Stokes number, $St_p = (1/18)(\rho_p/\rho_f)(D_p/\eta_0)^2 = 100$. Particle dynamics is based only on the drag force modeled using the standard Schiller-Naumann drag correlation. Keeping all the above parameters the same, the grid is systematically refined ($\Delta = 2\pi/96$, $2\pi/144$, $2\pi/192$, and $2\pi/256$), and simulations are carried out for the four different interpolation kernels described before. Thus, D_p/Δ ranges between 1–2.66 from the coarsest to the finest resolution. Initially, particles are injected at random positions and the particle velocity is set equal to the fluid velocity interpolated to the particle location using trilinear interpolation.

Figure 2(a,b) shows the temporal evolution of particle kinetic energy normalized by the initial fluid phase kinetic energy obtained using the grid-based Roma interpolation

$\frac{t\epsilon_0^{(f)}}{k_0^{(f)}}$	PR-DNS	PP-DNS (Trilinear)	E&H (Trilinear)	No Correction			Zonal-ADR		
				Roma	Gauss1 $\frac{\sigma}{D_p} = 0.8$	Gauss2 1.5	Roma	Gauss1 $\frac{\sigma}{D_p} = 0.8$	Gauss2 1.5
0.54	0.9303	0.9267	0.9246	0.9645	0.9410	0.9351	0.9236	0.9283	0.9279
2.7	0.5172	0.4732	0.4701	0.7028	0.5562	0.5272	0.4693	0.4977	0.5010
4.87	0.2855	0.2423	0.2453	0.5141	0.3331	0.3004	0.2483	0.2670	0.2743
6.55	0.1821	-	0.1562	0.4081	0.2302	0.1999	0.1564	0.1714	0.1754

TABLE 2. Normalized particle kinetic energy ($k^{(p)}/k_0^{(f)}$) at different times predicted with and without the Zonal-ADR model with different interpolation kernels and compared against PR-DNS as well as PP-DNS by Mehrabadi *et al.* (2018). E&H represents the implementation of the correction scheme by Esmaily & Horwitz (2018) in the present solver.

kernel for four different grid resolutions with and without any self-disturbance correction. Without any correction model, as the grid is refined, the prediction of particle kinetic energy becomes more inaccurate, a result consistent both with the stationary particle test case presented in Section 3.1 and with the conclusions of Horwitz & Mani (2020). As the grid is refined, the Roma interpolation kernel becomes narrow, adding a large reaction force in the neighborhood of the particle and creating a strong disturbance field. Since the fluid velocity is sampled using the same interpolation kernel and without any correction, the particle force is underpredicted, resulting in the slower decay of the particle kinetic energy. With the Zonal-ADR correction, however, all grid resolutions predict the temporal evolution of the particle kinetic energy very similar to the PR-DNS data. Thus, even for this grid-based, narrow interpolation kernel, the Zonal-ADR correction captures the fluid-particle interactions fairly accurately. The small mismatch compared to the PR-DNS data in Figure 2(b) is attributed to the lack of knowledge on the exact parameters for initial spectrum used in PR-DNS, and the use of a collocated grid-based solver in the present work.

The effect of using interpolation kernel widths proportional to the particle size is investigated next. Figure 3(a) shows the temporal evolution of normalized particle kinetic energy using the four interpolation kernels with and without the correction scheme on the 192^3 grid. Even without any correction, the kinetic energy decay rate is reasonably well captured by the Gauss1, Gauss2, and Roma-Gauss2 interpolation kernels. The kinetic energy is slightly overpredicted without correction. This is because the fluid velocity at the particle location contains the self-disturbance and results in a smaller particle force, similar to the stationary particle case. With correction, however, the results follow the PR-DNS study reasonably well for all interpolation kernels. Table 2 documents the particle kinetic energy at different times with and without the correction model for different interpolation kernels compared to the PR-DNS study. Also shown is the PP-DNS study conducted by Mehrabadi *et al.* (2018), using the correction scheme developed by Horwitz & Mani (2018), and predictions from the E&H correction scheme (Esmaily & Horwitz 2018) with trilinear interpolation implemented in the present solver.

Figure 3(b) shows the temporal evolution of the net dissipation rate normalized by the initial dissipation rate for the various interpolation kernels with and without correction. As shown by Sundaram & Collins (1996) and Mehrabadi *et al.* (2018), the evolution

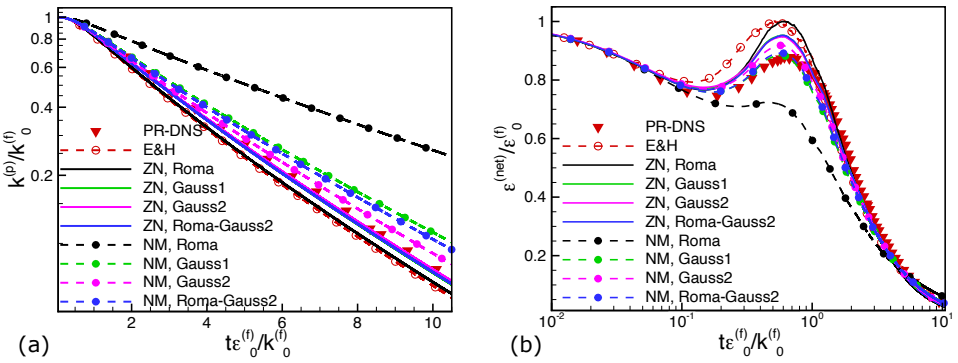

FIGURE 3. Temporal evolution of (a) normalized particle kinetic energy and (b) net dissipation rate using the Zonal-ADR model (ZN) and no model (NM) with different interpolation kernels on the 192^3 grid. The PR-DNS data Mehrabadi *et al.* (2018) and Esmaily & Horwitz (2018) correction scheme (E&H) with trilinear interpolation and implemented in this solver is also shown for comparison. The Gauss1 and Gauss2 lines for Zonal-ADR nearly overlap.

equation for the mixture kinetic energy of the system $e_m = (1-\phi)\rho_f k^{(f)} + \phi\rho_p k^{(p)}$ is

$$\frac{de_m}{dt} = \underbrace{(1-\phi)\frac{1}{V}\int_V \mu \mathbf{u}_f \nabla^2 \mathbf{u}_f dV}_{-\epsilon^{(f)}} + \underbrace{\frac{1}{V}\sum_{i=1}^{N_p} F_i \cdot (u_{p,i})}_{\Pi^{(p)}} - \underbrace{(1-\phi)\frac{1}{V}\sum_{i=1}^{N_p} F_i \cdot (u_{f@p,i})}_{\Pi^{(f)}}, \quad (3.1)$$

where F_i is the force acting on a particle, $-\epsilon^{(f)}$ is the kinetic energy dissipation rate resolved on the grid, $\Pi^{(p)}$ is the particle kinetic energy dissipation rate, and $\Pi^{(f)}$ is interphase kinetic energy transfer term between the particle and fluid. Here, $-\epsilon^{(*)} = \Pi^{(p)} - \Pi^{(f)}$ represents the additional dissipation near the particle surfaces (Sundaram & Collins 1996). In the present work, the net dissipation rate $[\epsilon^{(net)} = -\epsilon^{(f)} + \Pi^{(p)} - \Pi^{(f)}]$ is computed from the rate of change of the fluid and particle kinetic energy [left-hand side of Eq. (3.1)]. Without correction, the grid-based Roma interpolation significantly underpredicts the net dissipation rate. However, particle size–based interpolation kernels capture the trends of the PR-DNS data even without correction. The peak in the dissipation rate, created mainly by the no-slip conditions and resultant flow disturbance in PR-DNS, is also well captured by the point-particle model with correction. Figure 4 shows the contributions of the resolved dissipation rate and interphase energy transfer $[-\epsilon^{(f)} - \Pi^{(f)}]$, the particle kinetic energy dissipation rate to the net dissipation rate for two interpolation kernels (Gauss1 and Roma-Gauss2) with and without correction. All parts of the dissipation rate are well captured by the particle-based interpolation kernel, even with the asymmetric Roma-Gauss2 interpolation. This suggests that sampling fluid velocity from a region less perturbed by the self-disturbance of the particle compensates for the errors introduced by nonsymmetric interpolation in the kinetic energy conservation, especially when the particles are on the order of the grid resolution.

4. Conclusions

A two way–coupled point-particle model is used to evaluate the particle-turbulence interactions with and without correcting for the self-disturbance created by Kolmogorov-

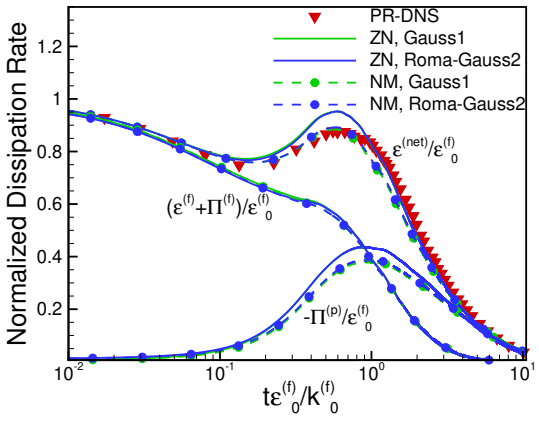

FIGURE 4. Temporal evolution of the resolved fluid ($-\epsilon^{(f)}$), particle dissipation rates ($\Pi^{(p)}$), and interphase energy transfer ($-\Pi^{(f)}$) to the net normalized dissipation rate ($\epsilon^{(net)}/\epsilon_0^{(f)}$) using the Zonal-ADR correction (ZN) and no model (NM) with different interpolation kernels.

scaled particles in decaying isotropic turbulence at low volume loading, corresponding to the PR-DNS data of Mehrabadi *et al.* (2018). A Zonal-ADR method (Apte 2022) is used for obtaining the undisturbed fluid velocity at the particle location needed for drag closure. Two types of interpolation kernels: (i) grid-based and (ii) particle-size based, are used to evaluate their influence on the particle-turbulence interactions. It is shown that the grid-based interpolation kernels, which vary based on the local grid resolution, irrespective of the particle size, significantly under predict the interaction force and hence the decay rates of particle kinetic energy, especially when no model is used for the self-disturbance correction. Particle-size based kernels with kernel widths that scale with the particle size can better capture these interactions even without any correction model. As the grid is refined and the particle size becomes larger than the grid resolution, a kernel width proportional to particle size keeps the region of particle-fluid interaction unchanged and allows sampling of the fluid parameters from a region that is less affected by the self-disturbance field. With correction for the self-disturbance field, all interpolation kernels resulted in a good prediction of the particle-fluid kinetic energy exchange. The particle kinetic energy decay rate is slightly under predicted with no correction model, suggesting the need for self-disturbance correction for particles comparable to the grid resolution. A detailed study at larger Reynolds numbers will be conducted in the future.

Acknowledgments

Computing time on Xsede's Frontera machine is appreciated. SVA and NK acknowledge NSF award#1851389. Authors thank Dr. J. Horwitz, Dr. M. Mehrabadi, and Prof. S. Subramaniam for the PR-DNS data.

REFERENCES

APTE, S. V. 2022 A zonal advection-diffusion-reaction model for self-disturbance correction in point-particle computations. *Proceedings of the Summer Program*, Center for Turbulence Research, Stanford University.

Apte, S.V., Gorokhovski, M. & Moin, P. 2003 LES of atomizing spray with stochastic modeling of secondary breakup. *Int. J. Multiph. Flow.* **29**, 1503–1522.

Deen, N. G., van Sint Annaland, M. & Kuipers, J. 2009 Direct numerical simulation of complex multi-fluid flows using a combined front tracking and immersed boundary method. *Chem. Eng. Sci.* **64**, 2186–2201.

Esmaily, M. & Horwitz, J. 2018 A correction scheme for two-way coupled point-particle simulations on anisotropic grids. *J. Comput. Phys.* **375**, 960–982.

Fukada, T., Fornari, W., Brandt, L., Takeuchi, S. & Kajishima, T. 2018 A numerical approach for particle-vortex interactions based on volume-averaged equations. *Int. J. Multiph. Flow.* **104**, 188–205.

Gualtieri, P., Picano, F., Sardina, G. & Casciola, C. M. 2015 Exact regularized point particle method for multiphase flows in the two-way coupling regime. *J. Fluid Mech.* **773**, 520–561.

Horwitz, J., Iaccarino, G., Eaton, J. & Mani, A. 2022 The discrete Green's function paradigm for two-way coupled Euler–Lagrange simulation. *J. Fluid Mech.* **931**, A3.

Horwitz, J. & Mani, A. 2016 Accurate calculation of Stokes drag for point–particle tracking in two-way coupled flows. *J. Comput. Phys.* **318**, 85–109.

Horwitz, J. & Mani, A. 2018 Correction scheme for point-particle models applied to a nonlinear drag law in simulations of particle-fluid interaction. *Int. J. Multiph. Flow* **101**, 74–84.

Horwitz, J. & Mani, A. 2020 Two-way coupled particle-turbulence interaction: Effect of numerics and resolution on fluid and particle statistics. *Phys. Rev. Fluids* **5**, 104302.

Liu, K., Lakhote, M. & Balachandar, S. 2019 Self-induced temperature correction for inter-phase heat transfer in Euler–Lagrange point-particle simulation. *J. Comput. Phys.* **396**, 596–615.

Lomholt, S., Stenum, B. & Maxey, M. 2002 Experimental verification of the force coupling method for particulate flows. *Int. J. Multiph. Flow.* **28**, 225–246.

Maxey, M. R. 1987 The gravitational settling of aerosol particles in homogeneous turbulence and random flow fields. *J. Fluid Mech.* **174**, 441–465.

Mehrabadi, M., Horwitz, J., Subramaniam, S. & Mani, A. 2018 A direct comparison of particle-resolved and point-particle methods in decaying turbulence. *J. Fluid Mech.* **850**, 336–369.

Paksereshт, P. & Apte, S. V. 2021 A disturbance corrected point-particle approach for two-way coupled particle-laden flows on arbitrary shaped grids. *J. Comput. Phys.* **439**, 110381.

Paksereshт, P., Esmaily, M. & Apte, S. V. 2020 A correction scheme for wall-bounded two-way coupled point-particle simulations. *J. Comput. Phys.* **420**, 109711.

Pope, S. B. 2000 *Turbulent Flows*. Cambridge University Press, Cambridge, MA.

Sundaram, S. & Collins, L. R. 1996 Numerical considerations in simulating a turbulent suspension of finite-volume particles. *J. Comput. Phys.* **124**, 337–350.